International Journal of Clinical Oncology and Cancer Research
2025, Vol. 10, No. 2, pp. 67-85
https://doi.org/10.11648/j.ijcocr.20251002.14

Research Article

Identification of Candidate Histone Lysine Lactylation (Kla)-associated Biomarkers in Lung Adenocarcinoma (LUAD) Via Integrated Bioinformatics Analysis

Yi Zhang[1], Jianhong Ren[2], Guangzhao Huang[3], Rurong Wang[1, 4, *]

[1]Department of Anesthesiology, West China Hospital, Sichuan University, Chengdu, China
[2]Department of Anesthesiology, Chengdu Shuangliu District Maternity Child Health Care Hospital, Chengdu, China
[3]Department of Head and Neck Oncology, West China Hospital of Stomatology, Sichuan University, Chengdu, China
[4]Department of Anesthesiology, Cheng Du Shangjin Nanfu Hospital, Chengdu, China

Abstract

Histone lysine lactylation (Kla), induced by lactate in tumor microenvironment, might be a novel therapeutic target for cancer. Lung adenocarcinoma (LUAD) was characterized by lactate accumulation in the TME. However, the role of histone Kla in lung LUAD is unclear. The RNA expression profile of LUAD was downloaded from The Cancer Genome Atlas (TCGA), and then selected differentially expressed Kla-specific genes (DEKlaGs), following building a prognostic model to predict the prognosis of patients with LUAD. On the other hand, we investigated the roles of prognostic biomarkers in the LUAD immune microenvironment, and determined its roles in the LUAD therapy response. Finally, the potential KEGG pathways influenced by histone Kla were investigated through gene set enrichment analysis (GSEA). A total of eighty-six DEKlaGs were identified with the cut-off criteria $\log_2 FC \geq 2$ and p-value<0.05. Four prognostic DEKlaGs, including C1QTNF6, HCN2, SLAMF9, and IL20RB, were enrolled in the Cox regression model. We showed that high expression of lactate production-associated genes was correlated with the expression of prognostic biomarkers. On the other hand, the activation of Kla was related to LUAD immune infiltration, and played a crucial role in LUAD drug resistance and immunotherapy resistance. Moreover, Kla was associated with the activation of MARK, NOTCH, JAK/STAT signaling pathways, and contributed to the focal adhesion of LUAD. In conclusion, C1QTNF6, HCN2, SLAMF9, and IL20RB induced by histone Kla might be crucial effective biomarkers for LUAD, suggesting that Kla was expected to be a novel therapeutic target for LUAD.

Keywords

LUAD, Lactate, Kla, Histone Lactylation, Immunotherapy, Prognosis

1. Introduction

Lung cancer is the second most prevalent cancer worldwide, with high mortality and unfavorable prognosis [1]. As the most common subtype of lung cancer, lung adenocarcinoma (LUAD) is characterized by high malignancy and the limited

*Corresponding author: wangrurong@scu.edu.cn (Rurong Wang)

Received: 8 April 2025; **Accepted:** 18 April 2025; **Published:** 19 May 2025

effectiveness of chemotherapy, which contribute to unsatisfactory overall survival [2]. Despite advances in treatment of LUAD, including immunotherapy, targeted therapy, and the identification of novel biomarkers in recent decades [3, 4], the overall prognosis of patients remains unfavorable, and one of the main reasons being the lack of efficient therapeutic targets [5]. Hence, deep understanding of the mechanism in LUAD therapy resistance and identification of effective biomarkers for LUAD are urgently required.

Epigenetic modifications directly enhance or inhibit gene activity without modifying the DNA sequence [6]. Histones are modified by various post-translational modifications, including methylation, acetylation, and phosphorylation, and thereby contribute to DNA compaction and regulate gene expression. In recent decades, aberrations in histone post-translational modifications have been identified to play a crucial role in cancer, both at the global level and across the genome [7, 8]. Zhao *et al.* identified that histone lysine lactylation (Kla) could directly regulate gene transcription from chromatin [9], and played a crucial role in the initiation and progression of malignant tumors [10]. Moreover, Kla may be associated with immunosuppression and therapy in various cancers [11, 12]. According to Zhao's study, Kla is induced by lactate derived from aerobic glycolysis, which is a characteristic of cancer cells [13]. Recently, Yu J and Wang *et al.* suggested that elevated levels of Kla might facilitate tumorigenesis, migration, and invasion in cancerss [14, 15]. Meanwhile, inhibition of histone Kla can suppress tumorigenicity induced by cancer stem cells [16]. In LUAD, activation of aerobic glycolysis is associated with tumorigenesis, chemoresistance, immune infiltration, and other processes. [17-19]. Moreover, lactate accumulation in the LUAD tumor microenvironment (TME) also plays a crucial role in immunotherapy [20]. Kla is sensitive to lactate level, while the roles of Kla in LUAD remain unclear.

In this study, we determined the prognostic value of histone Kla-specific genes (KlaGs) by building a Cox regression model. We also analyzed the correlation between lactate production-associated gene expression and prognostic Kla-specific gene expression. Meanwhile, we explored whether activation of histone Kla could induce the expression of prognostic biomarkers. On the other hand, we investigated the role of Kla in drug therapy and immunotherapy responses. Finally, we speculated the potential Kyoto Encyclopedia of Genes and Genomes (KEGG) pathways influenced by histone KlaGs in LUAD.

2. Material and Methods

2.1. Study Design and Data Collection

The LUAD gene expression profile and corresponding clinical data were downloaded from TCGA database (https://portal.gdc.cancer.gov). A total of 54 normal and 503 tumor cases were identified (https://portal.gdc.cancer.gov/projects/TCGA-LUAD). Twenty tumor samples were removed because of inadequate clinical data. Histone KlaGs were obtained from Zhao's study in 2019 [9] (https://www.ncbi.nlm.nih.gov/pmc/articles/PMC6818755/#SD4). Furthermore, differentially expressed KlaGs (DEKlaGs) were selected using the R software limma package, with the cut-off criteria $\log_2$FoldChange (FC) ≥ 2 and p-value<0.05. All patients in our study were obtained from public database. So, ethical approval and informed consent were not required in our study.

2.2. Identification of Kla Prognostic Value

Univariate Cox regression analysis was used to select prognostic DEKlaGs with the cut-off criteria p-value<0.05. Furthermore, prognosis-associated DEKlaGs were enrolled in multivariate Cox regression analysis, and then step-wise Cox regression analysis was used to construct a risk model. Subsequently, the patients were divided into high- and low-risk groups according to the median of risk score which was calculated by gene expression in line with the risk model. Kaplan-Meier curves along with long-rank test were used to determine the prognosis of the two groups. Meanwhile, the risk score combined with gene expression and survival time was visualized in R software. Moreover, the prognostic values of genes enrolled in Cox model were further also identified by survival analysis.

2.3. Correlation Analysis Between Kla Related Genes and DEKlaGs

According to Zhao's study [9], the E1A binding protein p300 (*P300*), hypoxia inducible factor 1 subunit alpha (*HIF1A*), lactate dehydrogenase A (*LDHA*), and lactate dehydrogenase B (*LDHB*) are related to lactate accumulation in the tumor microenvironment (TME) and all play a critical role during the histone Kla process. Therefore, we explored the correlation between these four genes and the KlaGs involved in the Cox model, including C1QTNF6, HCN2, SLAMF9, and IL20RB.

2.4. Drug Susceptibility Analysis

To explore the role of Kla in LUAD drug therapy, we downloaded drug susceptibility data from the Cellminer database [21] (https://discover.nci.nih.gov/cellminer/home.do), and then investigated the correlation between prognostic KlaGs and drug susceptibility. Briefly, sixty patients and their corresponding gene expression profiles and drug susceptibility data were obtained from Cellminer database. Furthermore, the expression level of prognostic KlaGs and drug therapy data of each patient were extracted. Finally, Pearson correlation analysis was used to evaluate the relationship between KlaGs and drug susceptibility. The top 3 drugs were listed.

2.5. Immune Infiltration Analysis

Based on the gene expression profile, we evaluated the im-

mune cell level in each sample using the R software "CIBERSORT" package. We then determined the correlation between prognostic KlaGs and the levels of immune cells. In addition, we further calculated the immune scores of LUAD patients in R software packages "GVSA" and "GSEAbase." According to the median of DEKlaGs expression, patients were divided into high- and low-expression groups, and then the difference in immune cell levels between the two groups was assessed.

2.6. Immunotherapy Analysis

First, we downloaded tumor mutation burden (TMB) from UCSC Xena (https://xena.ucsc.edu/). TMB is regarded as an indicator for predicting response to immunotherapy [22]. Therefore, we explored the correlation between TMB levels and DEKlaGs. Furthermore, we obtained immunotherapy data for LUAD patients from the TCIA database (https://tcia.at/home) [23]. We further investigated the role of Kla in LUAD immunotherapy. Meanwhile, we investigated the expression correlation between KlaGs and immune checkpoints obtained from a previous study [24].

2.7. Gene Set Enrichment Analysis (GSEA)

To explore the role of Kla in the initiation and progression of LUAD, we determined the potential mechanisms influenced by Kla using gene set enrichment analysis (GSEA) (https://www.gsea-msigdb.org/gsea/index.jsp) [23]. In short, patients were divided into high (H) and low (L) groups in accordance with the median of gene expression. Furthermore, the group file and gene expression file were uploaded in GSEA software to select pathways influenced by Kla. The L group was the control, and KEGG was selected as gene set in the software. The top 3 KEGG pathways are listed below.

2.8. Statistical Analysis

Pearson's Correlation Tests, Student's t-test and log-rank test were carried out in SPSS software (Version 23.3, IBM) ($p<0.0001$****; $p<0.001$***; $p<0.01$ **; $p<0.05$ *).

3. Results

3.1. Histone Kla Was Correlated to Unsatisfied Prognosis of LUAD

To investigate the prognostic value of histone Kla in LUAD, we identified DEKlaGs and then constructed a Cox model. According to differentially expressed analysis, a total of 86 DEKlaGs were identified (Figure 1A, B, Table A1). Univariate Cox analysis indicated that eight genes might be candidate biomarkers in LUAD (Table 1). Multivariate Cox regression combined with stepwise regression analysis was used to construct a risk model based on these eight prognostic genes (Figure 1C). Risk-scores of each patient were calculated on basis of C1q and TNF-related 6 (C1QNTF6), hyperpolarization-activated cyclic nucleotide gated potassium and sodium channel 2 (HCN2), interleukin 20 receptor subunit beta (IL20RB), and SLAM family member 9 (SLAMF9) expression, and then patients were divided into high- and low-risk groups according to the median risk score. Survival analysis showed that patients with high-risk score had lower overall survival (Figure 1D). In addition, the survival analysis also suggested that high expression of these four genes also contributed to unsatisfied overall survival (Figure A1 A-D). Furthermore, risk score was further identified as an independent prognostic biomarker for LUAD (Figure 1E, F). Receiver operating characteristic (ROC) curve also, to some extent, suggest the accuracy of risk model (Figure A1E). Subsequently, we visualized the risk model combined with gene expression and survival time using the R software (Figure 1G). Furthermore, survival analysis combined with clinical parameter stratification analysis indicated that the risk model might accurately predict LUAD prognosis (Figure 1H, I). These results suggested that histone Kla played a crucial role in LUAD prognosis.

Table 1. *Univariate cox analysis based on KlaGs.*

Gene	HR	HR.95L	HR.95H	coxPvalue
C1QTNF6	1.0276	1.0183	1.0370	0.0000
EGLN3	1.0032	1.0010	1.0055	0.0053
GINS4	1.0300	1.0038	1.0569	0.0247
HCN2	1.0404	1.0041	1.0781	0.0290
IL20RB	1.0074	1.0033	1.0115	0.0004
SLAMF9	1.0419	1.0202	1.0641	0.0001
SUSD2	0.9988	0.9978	0.9998	0.0210
TUBB3	1.1277	1.0176	1.2498	0.0219

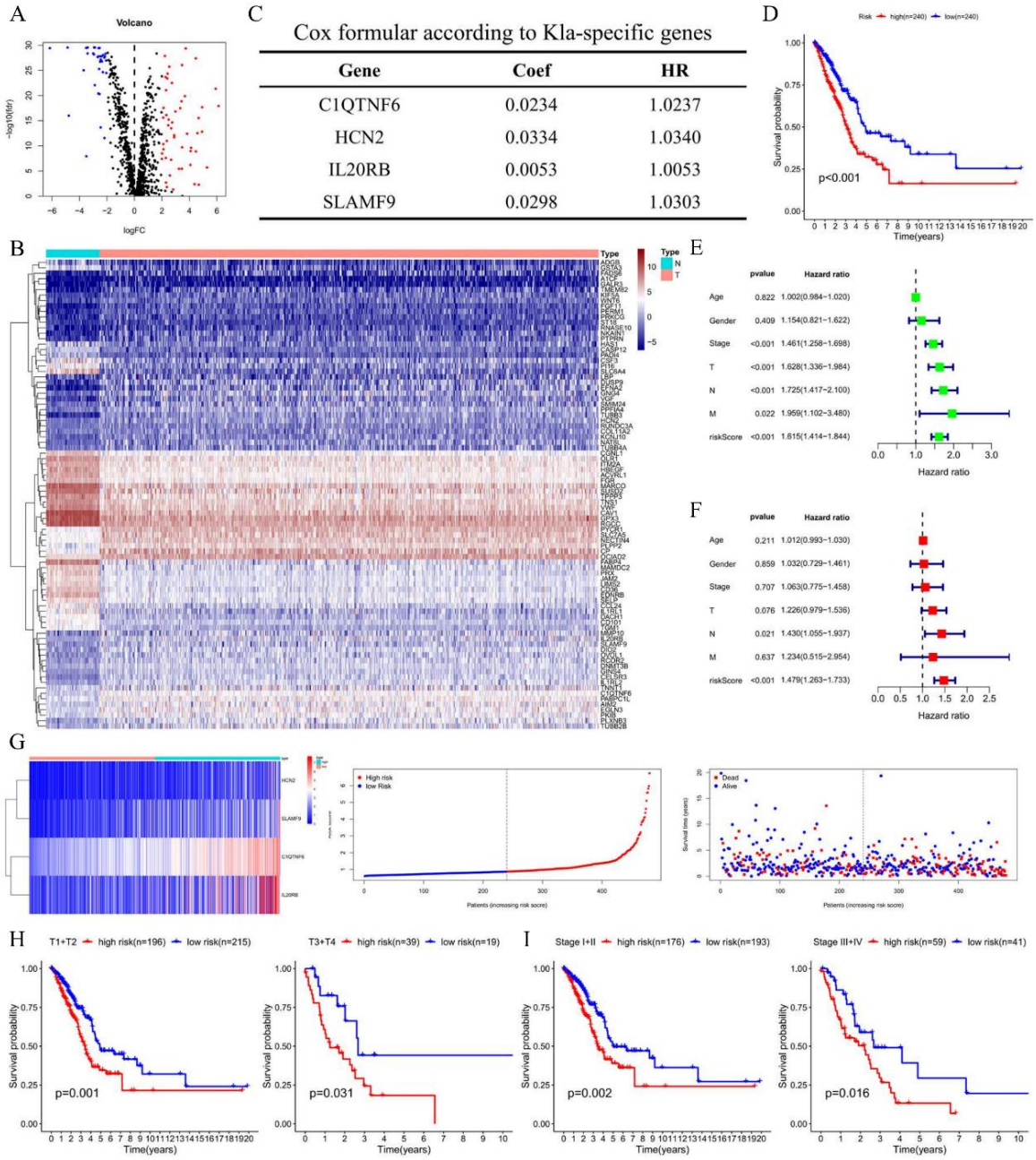

Figure 1. *Histone Kla was related to the prognosis of LUAD. A, The volcano map of differentially expressed Kla-specific genes (DEKlaGs) in LUAD. Histone Kla-specific genes (KlaGs) were obtained from Zhao's study following differentially expressed analysis with the cut-off criteria log2FC≥2, p-value<0.05. Blue represents downregulated genes, while red represents upregulated genes. FC: foldchange. B, The heat map of differentially DEKlaGs in LUAD. N: normal samples, T: tumor samples. C, Multivariate Cox regression analysis was used to build a Cox model in line with DEKlaGs. D, Survival analysis based on risk score of each LUAD patient. E, Univariate analysis suggested that risk score in line with DEKlaGs might be a potential candidate biomarker for LUAD. T: Tumor size, N: lymph node metastasis. M: distant metastasis. F, Multivariate analysis showed that risk score in line with DEKlaGs might be an independent prognostic biomarker in LUAD. G, Risk score along with gene expression and survival time was visualized in R software. H; I, Survival analysis according to T classification and clinical stage of LUAD. Kla: lysine lactylation.*

3.2. Histone Kla Might Be a Novel Indicator for Advanced LUAD

To further determine the role of histone Kla in LUAD, we investigated the difference in prognosis-associated KlaGs and risk score between early and advanced LUAD cases. Unfortunately, prognosis-associated genes had no effect on TNM stage and clinical stage (Figure 2A-D). We further explored the prognostic value of risk score model, a combination of prognosis-associated KlaGs. We suggested that high risk

score levels mean larger tumor size, elevated potential for lymph node and distant metastasis. Meanwhile, the risk score of LUAD patients in the advanced stage was remarkably higher than the early stage (Figure 2E). Hence, the risk score associated with Kla might be an indicator for high TNM stage and advanced clinical stage in LUAD. These observations showed that histone Kla might be a candidate biomarker for advanced LUAD cases.

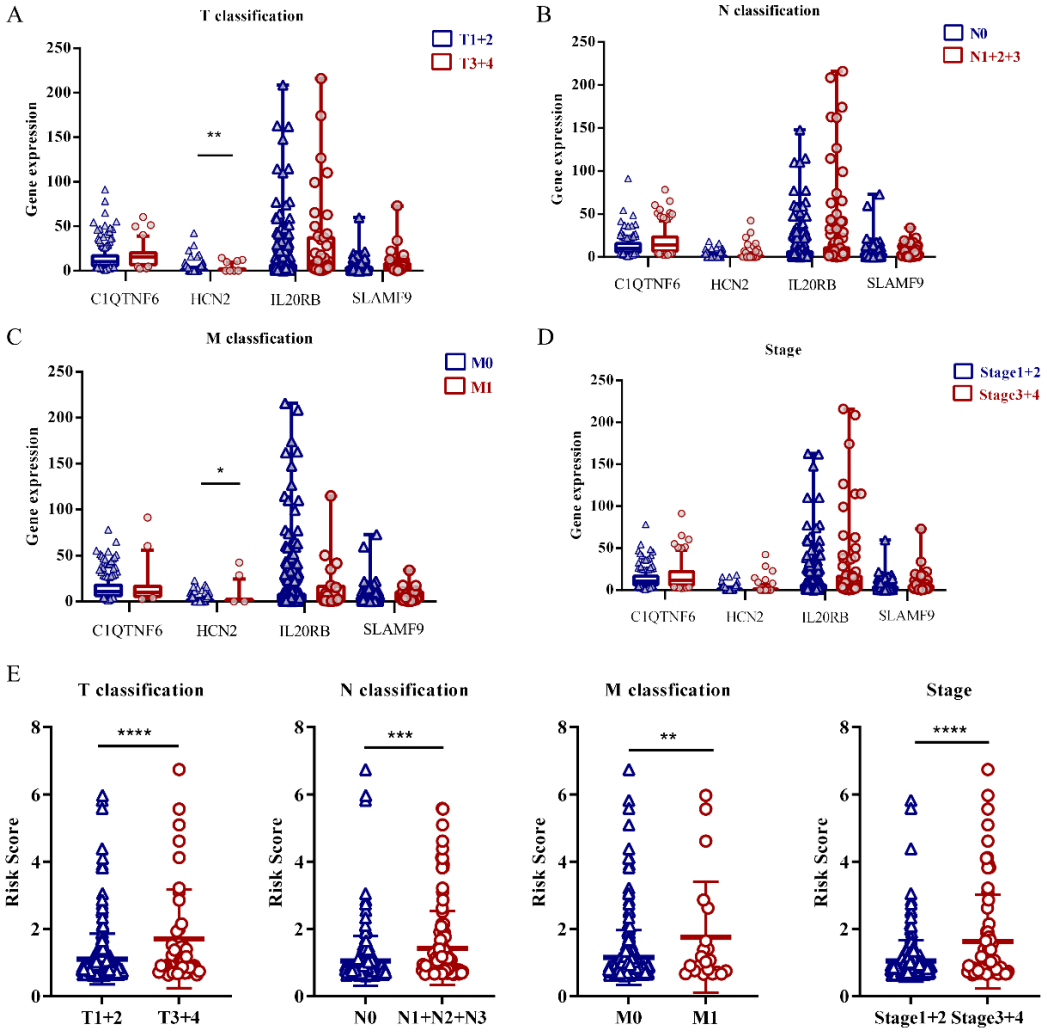

Figure 2. *Risk-score based on histone KlaGs might be an indicator for advanced LUAD cases. A, The correlation between tumor size and C1QTNF6, HCN2, SLAMF9, and IL20RB expression. B, The correlation between lymph node metastasis and C1QTNF6, HCN2, SLAMF9, and IL20RB expression. C, The role of C1QTNF6, HCN2, SLAMF9 and IL20RB in LUAD distant metastasis. D, The correlation between clinical stage and C1QTNF6, HCN2, SLAMF9, and IL20RB expression. E, High-risk score might be an indicator for large tumor size, high potential for lymph node and distant metastasis, and advanced clinical stage.*

3.3. Lactate Accumulation Was Correlated with KlaGs Expression in LUAD

To explore whether the expressions of DEKlaGs could be induced by lactate in the TME, we obtained the expression of P300, HIF1A, LDHA, and LDHB, which have been identified to play a crucial role during the Kla process, and then investigated the correlation between lactate accumulation and DEKlaGs expressions. As the results show, the mRNA levels of HIF1A, LDHA, and LDHB were elevated in LUAD cases obtained from TCGA (Figure 3A). On the other hand, we showed that P300 was positively correlated with C1QTNF6 and HCN2 expression and negatively correlated with SLAMF9 expression (Figure 3B). HIF1A and LDHA induced four prognostic Kla-specific gene expressions in LUAD (Figure 3C, D). Similarly, LDHB positively correlated with C1QTNF6, HCN2, and IL20RB expression (Figure 2E), suggesting that lactate production in the TME might mediate C1QTNF6, HCN2, SLAMF9, and IL20RB expression. These observations indicated that lactate might mediate the expression prognostic molecules.

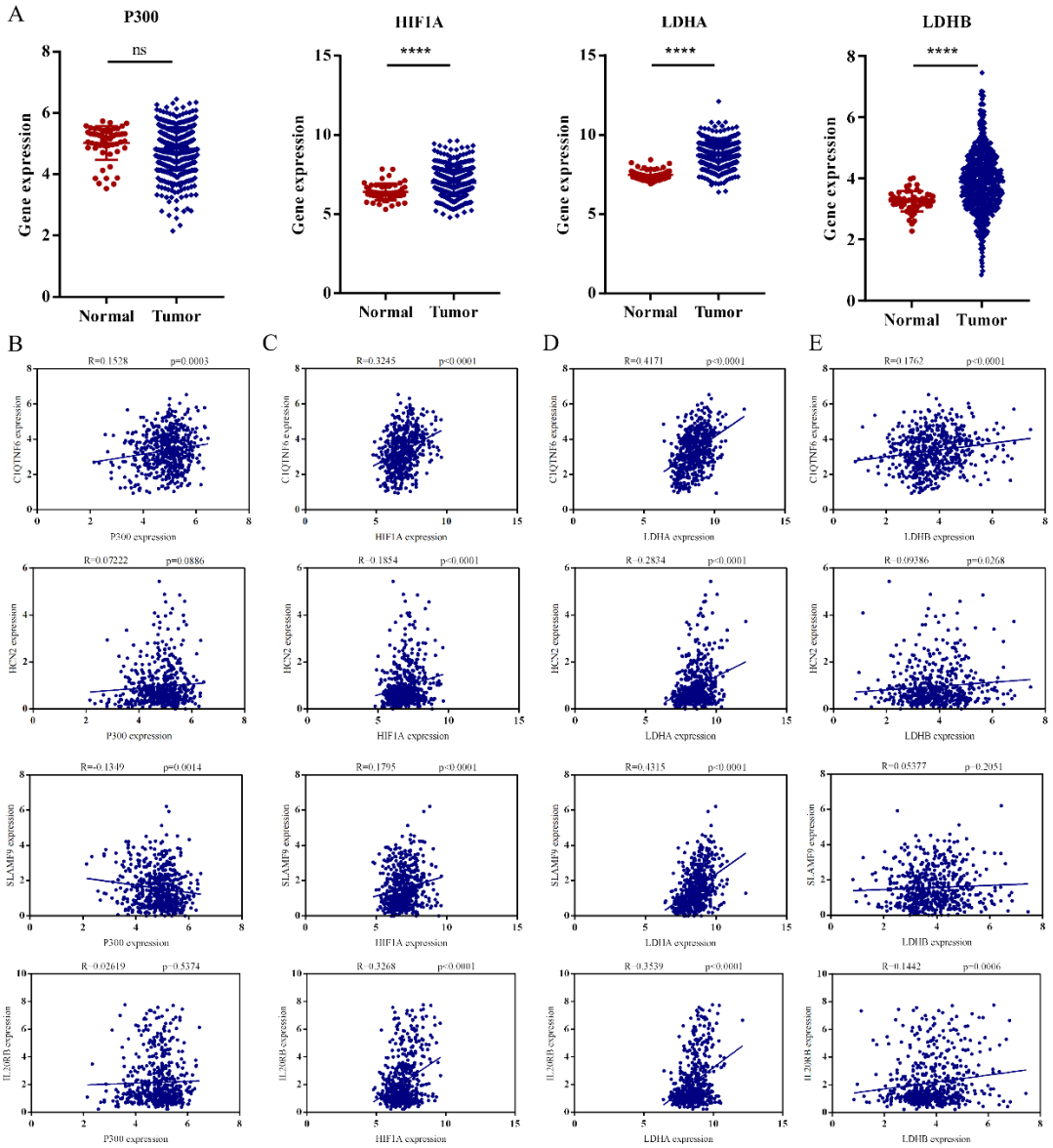

Figure 3. *Lactate accumulation induced the expression of prognostic Kla-specific gene expression. A, The mRNA expression of P300, HIF1A, LDHA and LDHB in LUAD. B, P300 was positively related to C1QTNF6 expression. C, HIF1A, which played a crucial role in aerobic glycolysis and lactate production, promoted all prognostic Kla-specific gene expression in LUAD. D; E, High expression of LDHA and LDHB might induce prognostic Kla-specific gene expression.*

3.4. Histone Kla Was Related to LUAD Immune Infiltration

To explore the role of histone Kla in LUAD TME, we further investigated the role of Kla in LUAD immunity. We found that the risk score was negatively related to the iDCs score and positively related to Treg score (Figure 4A). Meanwhile, high risk score might lead to undesirable Type-2 IFN response (Figure 4B). These results indicated that histone Kla plays a crucial role in LUAD immune infiltration and the Type-2 IFN response. The correlation analysis between prognostic KlaGs and immune scores were further conducted. High C1QTNF6 expression was associated with elevated Treg function and low Type-2 IFN response (Figure A2A). HCN2 might play a crucial role in regulating the function of follicular helper T cell (Tfh) and enhanced Treg function (Figure A2B). SLAMF9 mainly regulated the different stages of Macrophages and inhibited the Type-2 IFN response (Figure A2C). However, the role of IL20RB in LUAD was faint (Figure A2D). Moreover, we investigated the role of C1QTNF6, HCN2, SLAMF9, and IL20RB in the relative infiltration patterns of immune cells. C1QTNF6 was positively related to the infiltration of M0 macrophages, resting NK cells, and Tregs, and negatively related to NK cell activation, resting mast cells, and resting dendritic cells (Figure

4C). HCN2 promoted Macrophage M1, Tregs and inhibited dendritic cell activation (Figure 4D). SLAMF9 played a crucial role in Macrophage M2 levels (Figure 4E), and IL20RB was associated with the activation of several immune cells, such as T cell CD4 memory (Figure 4F). These findings suggested that histone Kla might exert a significant influence on immune infiltration within LUAD.

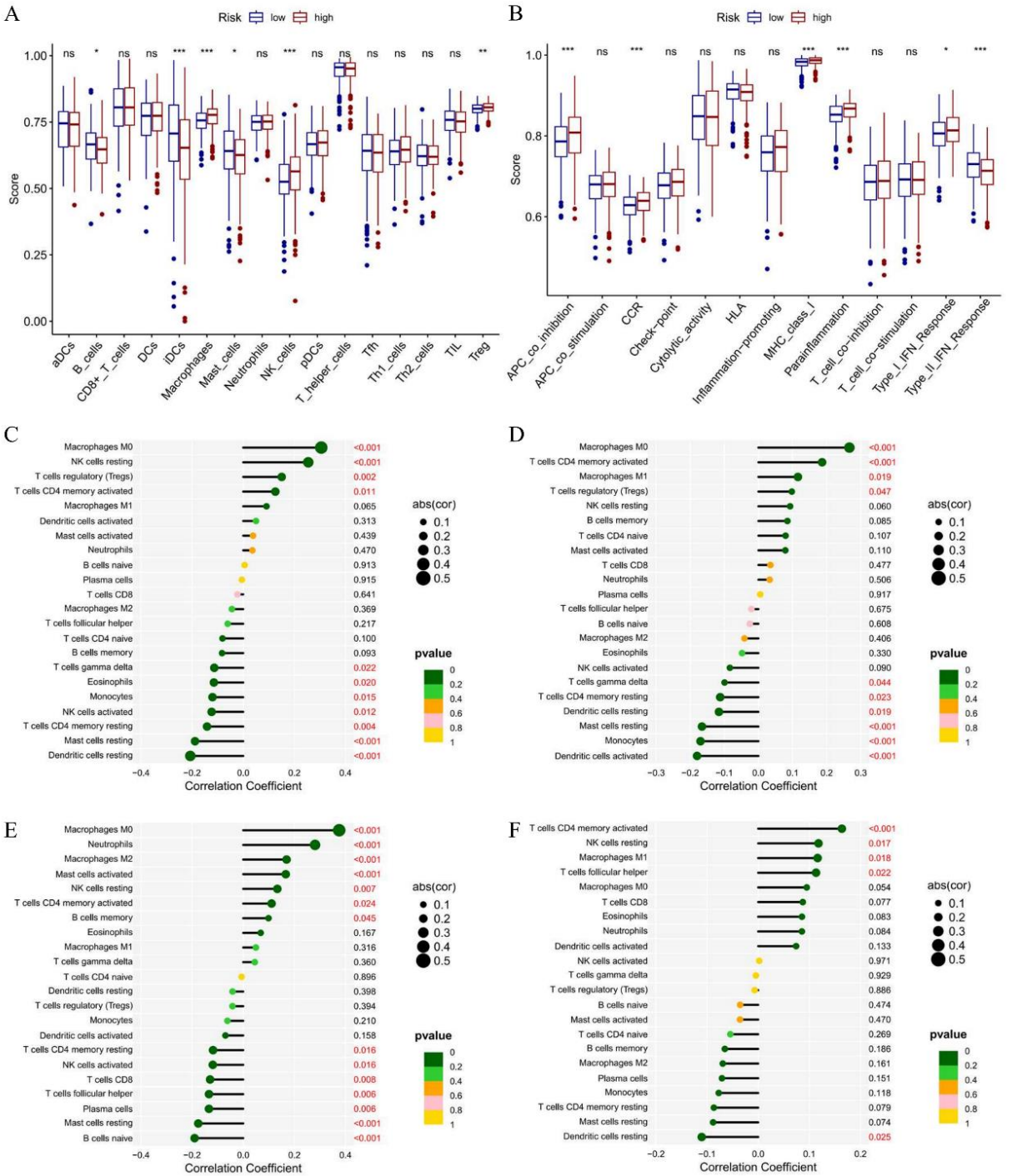

Figure 4. *Prognostic KlaGs were related to LUAD immune infiltration. A, The risk score was negatively related to the iDCs score and positively related to Macrophage and Treg score. B, High risk score meant undesirable Type-2 IFN response. C, High C1QTNF6 expression is related to high level of Tregs, low activated NK cells and memory T cells infiltration. D, High HCN2 also meant high Tregs level. E, SLAMF9 is related to LUAD tumor associated macrophage infiltration and lower T cells, B cell, and NK cells. F, IL20RB is positively related to T cells CD4 memory activated.*

3.5. C1QTNF6, HCN2, SLAMF9, and IL20R Inhibited the Immunotherapy Response of LUAD

We further explored the role of Kla in LUAD immunotherapy. TMB serves as an indicator for the prediction of the immune therapy response. High expression of C1QTNF6, HCN2, SLAMF9, and IL20RB was positively associated with TMB level (Figure 5A-D), suggesting that these molecules might be novel immunotherapeutic targets for LUAD. In addition, co-expression analysis showed that Kla activation was correlated with majority of immune checkpoints, such as CD28, CD276, TNFSF15, etc. (Figure 5E). Furthermore, we obtained immunotherapy data for LUAD from the TCIA. Differential analysis demonstrated that high C1QTNF6, HCN2, SLAMF9, and IL20RB levels were negatively correlated with four types of IPS scores (Figure 5F-I). These results indicated that C1QTNF6, HCN2, SLAMF9, and IL20RB might be critical immunotherapy targets for LUAD.

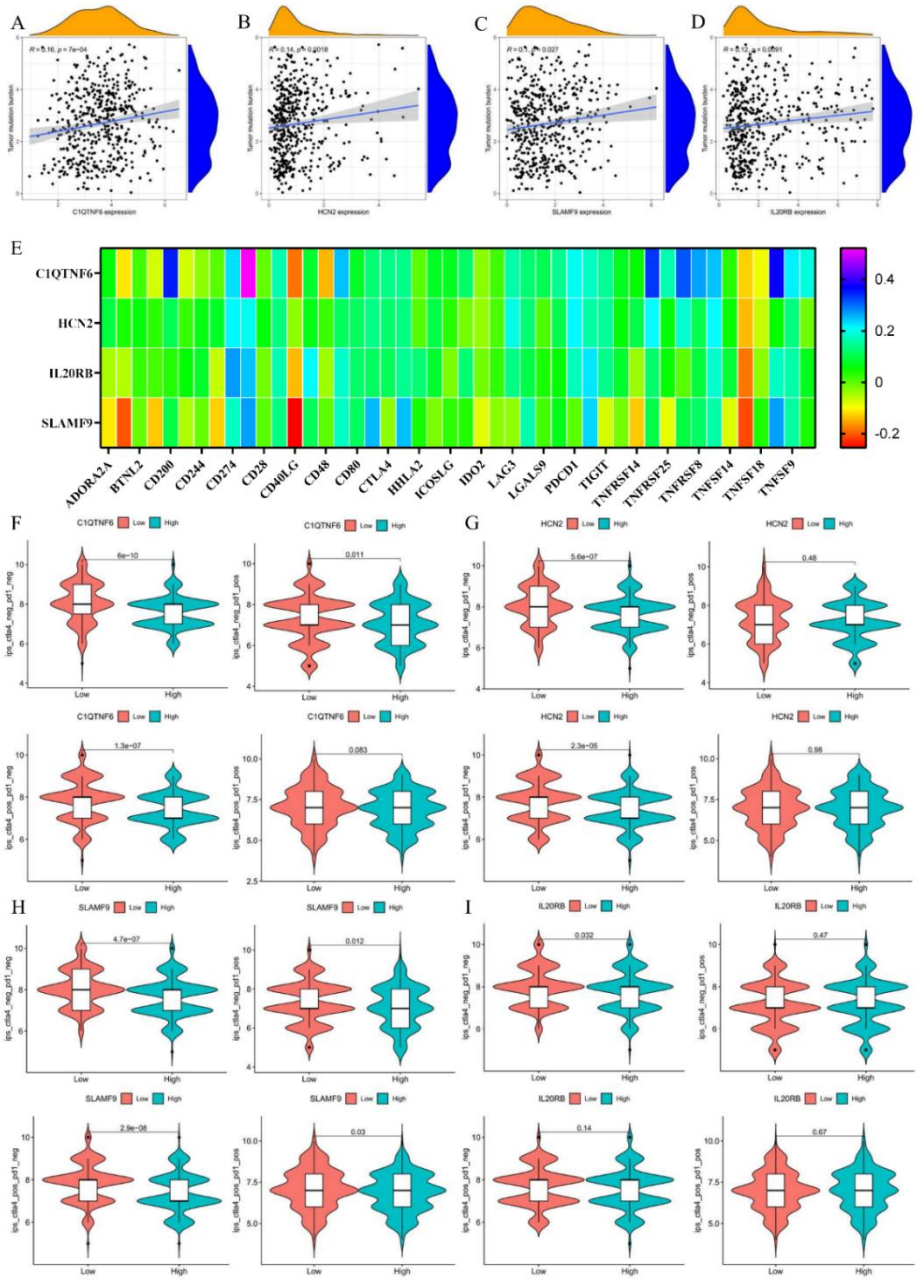

Figure 5. *Histone Kla inhibited the immunotherapy response of LUAD. C1QTNF6 (A), HCN2 (B), SLAMF9 (C) and IL20RB (D) are positively related to high TMB level of LUAD. E, Expression correlation between KlaGs and immune check point obtained from previous studies. F-I, The role of C1QTNF6, HCN2, SLAMF9 and IL20RB on LUAD immunotherapy response including ctla4-neg-pd1-neg, ctla4-neg-pd1-pos, ctla4-pos-pd1-neg and ctla4-pos-pd1-pos.*

3.6. C1QTNF6, HCN2, SLAMF9, and IL20R Were Related to LUAD Drug Resistance

To evaluate the role of Kla in drug therapy, we downloaded drug susceptibility data and determined the correlation between drug susceptibility and DEKlaGs (Table A2-A5). The results showed that activation of Kla was associated with drug resistance in LUAD. High levels of C1QTNF6 were associated with lower susceptibility to drugs such as Carfilzomib, Pipamperone, etc. (Figure 6A). HCN2 impaired the response to MEK1/2 inhibitors such as selumetinib (Figure 6B). Similarly, SLAMF9 and IL20RB showed remarkable drug resistance (Figure 6C, D). These results showed that targeting Kla might be helpful for LUAD drug therapy.

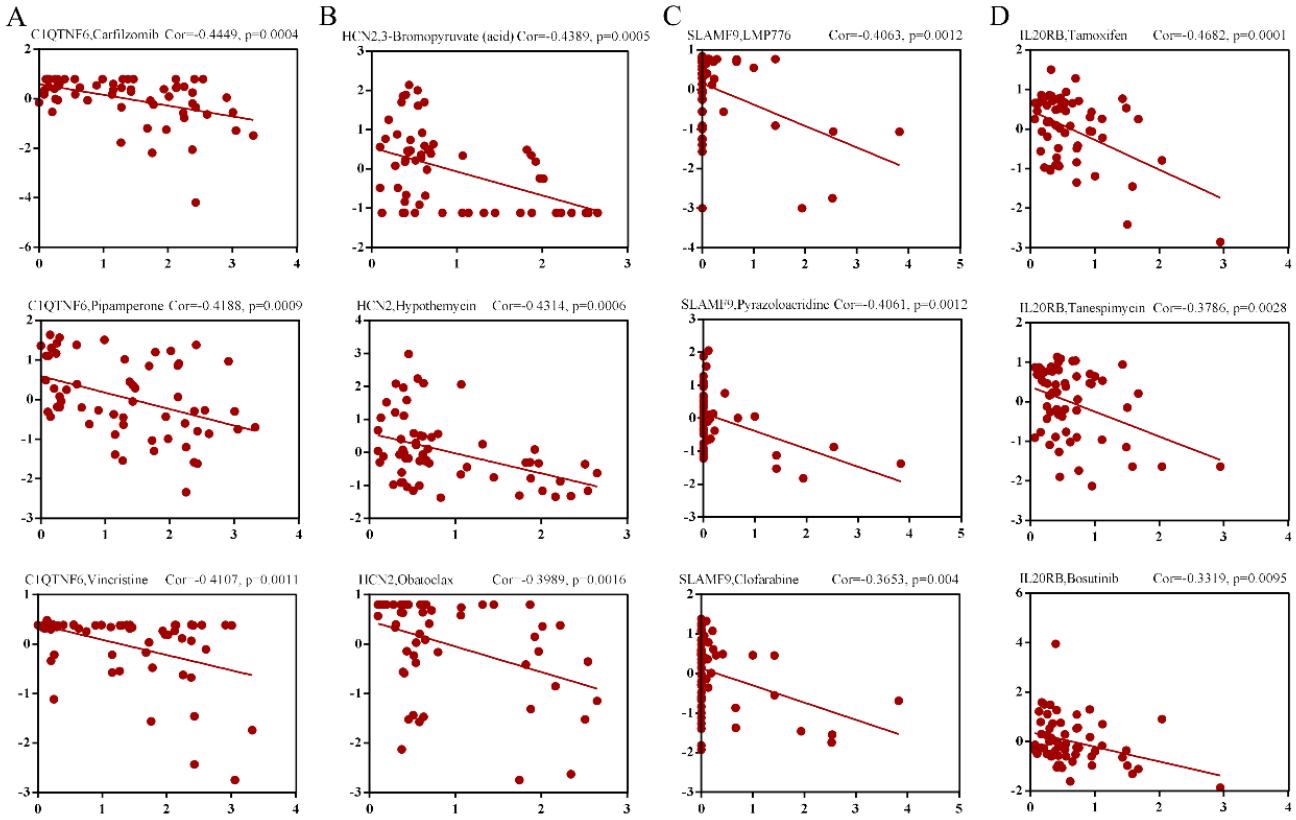

Figure 6. *C1QTNF6, HCN2, SLAMF9 and IL20RB might induce LUAD drug resistance. A, The high expression of C1QTNF6 was related to unsatisfied response to Carfilzomib, Pipamperone and etc. B, HCN2 induced LUAD 3-Bromopyruvate (acid) resistance. C, SLAMF9 was positively associated with lower drug susceptibility of Clofarabine. D, IL20RB might mediate the resistance of Tamoxifen and Bosutinib.*

3.7. C1QTNF6, HCN2, SLAMF9, and IL20RB Contribute to LUAD-associated Pathways Activation

To explore the potential pathways influenced by Kla, we performed gene set enrichment analysis to screen for potential KEGG pathways. C1QTNF6, HCN2, SLAMF9, and IL20RB all contributed to the activation of the cell cycle and focal adhesion pathways (Figure A3), suggesting that histone Kla might play a crucial role in LUAD proliferation and EMT. Furthermore, our results demonstrated that C1QTNF6 and HCN2 could activate the MAPK, NOTCH, and VEGF signaling pathways (Figure 7A, B), which play vital roles in tumorigenesis and metastasis. In addition, SLAMF9 was related to several metabolic pathways, such as the citrate cycle, TCA cycle, and glycolysis gluconeogenesis (Figure 7C). IL20RB was significantly associated with the immune response pathways (Figure 7D). These results indicated that histone Kla might promote LUAD progression and therapy resistance through these signaling pathways.

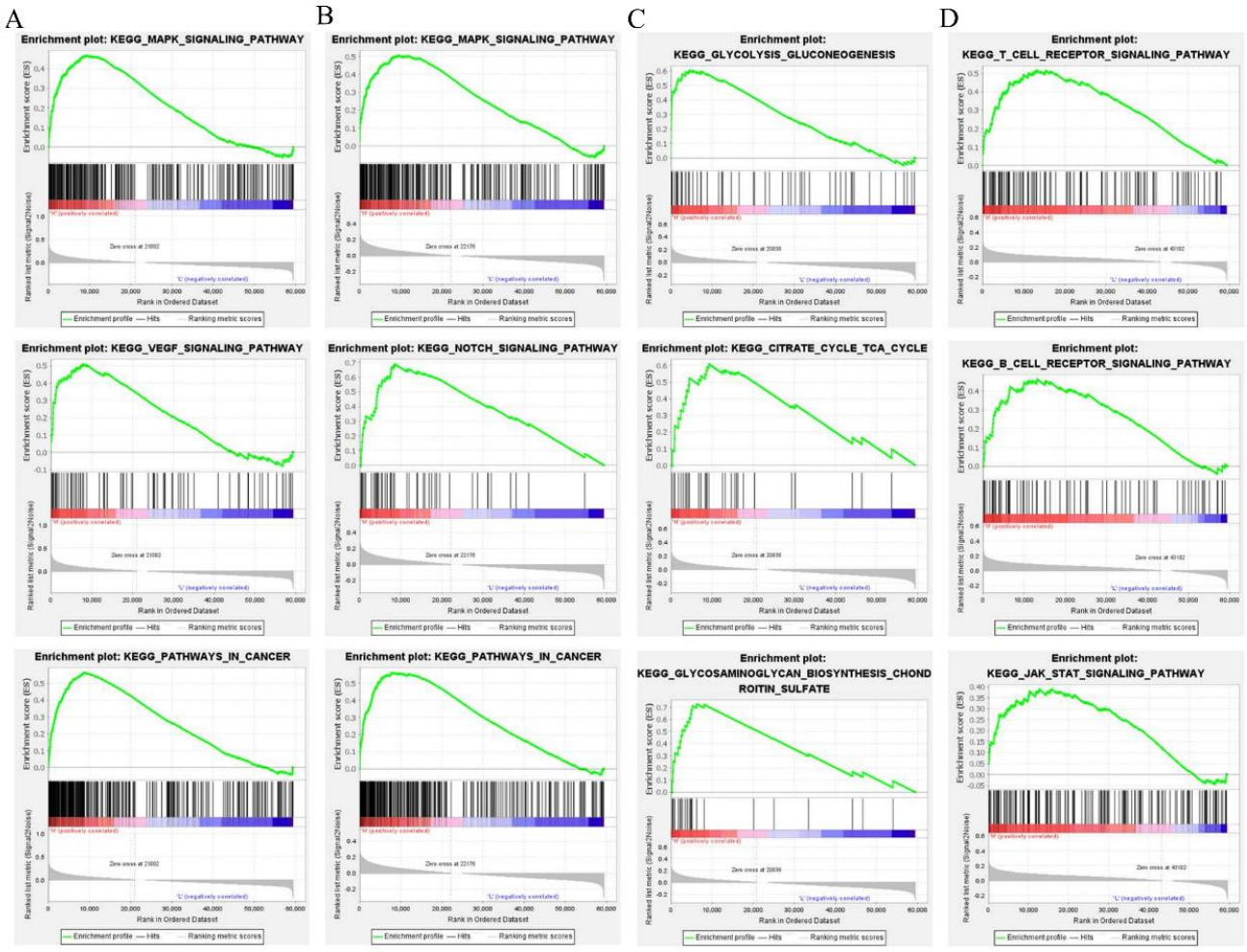

Figure 7. *Prognostic Kla specific genes promoted the activation of various LUAD-associated KEGG pathways. A; B, C1QTNF6 and HCN2 were associated with the activation of MAPK, VEGF and NOTCH signaling pathways. C, SLAMF9 might induce the dysregulation of metabolic pathways. D, IL20RB was related immune response pathways and JAK/STAT signaling pathway.*

4. Discussion

Aerobic glycolysis is the result of cancer cell reprogramming of metabolic pathways, leading to lactate accumulation in the TME [24], which contributes to cancer invasion and metastasis [25]. Moreover, lactate can inhibit the immune response and tumor surveillance mediated by T and NK cells, and thereby lead to tumor immune escape [26, 27]. LUAD is characterized by the activation of aerobic glycolysis, which enhances LUAD progression and immunosuppression [28, 29]. Lactate, the primary byproduct of aerobic glycolysis, contributes to unfavorable immunotherapy efficacy and poor prognosis in patients with LUAD [30]. However, whether Kla induced by lactate derived from aerobic glycolysis plays a key role in LUAD remains unclear. Hence, we investigated the prognostic role of Kla in LUAD.

In the present study, we found that the risk value calculated using KlaGs could accurately predict the prognosis of LUAD patients and might serve as an independent prognostic biomarker. Four oncogenes, including C1QTNF6, HCN2, SLAMF9, and IL20RB, were identified as candidate therapeutic targets for LUAD. C1QTNF6, as an inflammation associated gene, was associated with the biological characteristics of tumors, and played a vital role in immune infiltration and drug sensitivity in pan-cancer studies, suggesting that it may be an effective prognostic biomarker [31]. We found that C1QTNF6 was overexpressed in LUAD, and patients with high C1QTNF6 expression showed remarkably unfavorable overall survival. Meanwhile, lactate in the LUAD TME might induce C1QTNF6 expression, indicating that C1QTNF6 may play a key role during the LUAD histone Kla process. Moreover, C1QTNF6 was positively related to Tregs, which are involved in cancer immunosuppression [32]. C1QTNF6 could regulate macrophages at different stages. Zhu et al. demonstrated that C1QTNF6 was related to macrophage infiltration, which played a crucial role in the unsatisfied prognosis of patients with LUAD [33]. C1QTNF6 as a tumor associated macrophages (TAMs)-related-genes con-

tributed to the poor prognosis of patients. Chen et al. also identified that C1QTNF6 was related to LUAD tumor immunity, and negatively associated with the abundance of M1 macrophages [34], suggesting that C1QTNF played a crucial role in LUAD immune infiltration. On the other hand, LUAD is characterized by chemotherapy resistance. For instance, cancer cell could impair cisplatin-induced endoplasmic reticulum stress and then contribute to cisplatin-resistance [35]. We suggested that C1QTNF6 induced by histone Kla attenuated the susceptibility to chemotherapy. Meanwhile, inhibition of C1QTNF6 expression suppressed LUAD proliferation and progression [36]. C1QTNF6 could also protect against ferroptosis to drive lung cancer progression and metastasis, suggesting that targeting C1QTNF6-associated ferroptosis could be a candidate strategy for lung cancer therapy [37]. Taken together, C1QTNF6 showed promise as a novel therapeutic target for LUAD. Our study showed that HCN2, mainly expressed in the brain and heart, is overexpressed in LUAD tumor tissues and associated with poor prognosis. Recently, Mok et al. suggested that HCN2 inhibition combined with chemotherapy might be a new treatment regimen for breast cancer [38]. Similarly, we found that HCN2 was associated with LUAD drug resistance. HCN2 played a crucial role in regulating macrophage polarization and enhancing immunotherapy resistance. Unfortunately, no study has explored the potential mechanism of HCN2 in the TME of LUAD. Further studies were required to determine its role. SLAMF9, associated with innate and adaptive immune responses [39]. We suggested that SLAMF9 was upregulated and related to unfavorable overall survival. High SLAMF9 levels were positively correlated with the level of Macrophage M2, which contributed to TME inflammatory reprogramming, malignancy, and metastasis in LUAD [40, 41]. SLAMF9 plays a vital role in liver inflammation by regulating TLR4 expression in macrophages [42]. On the other hand, SLAMF9 inhibited the response of patients with LUAD to immunotherapy and drug therapy, suggesting that SLAMF9 might be an effective therapeutic target for LUAD. Recently, SLAMF9, identified in TAMs, was shown to influence pro-inflammatory cytokine secretion and migration in melanoma [43]. In clear cell renal cell carcinoma (ccRCC), SLAMF9 was regarded as an indicator for the progression and prognosis of patients [44]. Reversing of docetaxel resistance might be a crucial treatment for LUAD [45]. Chen et al. showed that the post-transcriptional modification of histone H3 lysine27 was associated with LUAD docetaxel resistance [46]. As the newly identified post-transcriptional modification, histone Kla could induce SLAMF9 expression, which played a crucial role in LUAD immune infiltration and enhanced docetaxel resistance, suggesting that SLAMF9 could serve as a promising therapeutic target. Lactate-induced expression of IL20RB was overexpressed in LUAD and promoted LUAD drug resistance. Generally, IL20RB and IL20RA always form a heterodimeric receptor that binds to IL-20 subfamily cytokines and then activates the intracellular JAK1/STAT3 signaling pathway [47]. Zhang et al. demonstrated that higher expression of IL20RB decreased the overall survival rate of patients [48]. Previous studies have shown that IL20RB, with its high prediction accuracy and stability in identifying immune features, could predict LUAD prognosis [49], which is similar to our study. In addition, IL20RB could influence the tumoral response to osteoclastic niches and promote bone metastasis in lung cancer [48]. In ccRCC, IL20RB was associated with poor prognosis and regulated immune cell infiltration. In our study, we also suggested that IL20RB was associated with immune cell infiltration in LUAD. Fan et al. indicated that IL20RB showed promise as a potential predictor of immunotherapy response to realize individualized treatment of LUAD [50]. Immunotherapy is regarded as an effective therapeutic method for lung cancer [51], LUAD is characterized by immune resistance [52]. TMB is the number of somatic coding mutations per million bases [53], which could be used to predict the immunotherapy response to immune checkpoint blocking (ICB) and survival outcomes in various cancers [54]. We suggested that prognostic KlaGs were positively related to the TMB level of LUAD. Bioinformatics analyses revealed that these genes induced by Kla played an important role in LUAD TME, drug resistance, and immunotherapy response, showing that histone Kla is a promising novel therapeutic target for LUAD. To explore the potential mechanism influenced by Kla, we performed GSEA in line with prognostic KlaGs. Activation of Kla might promote the cell cycle and enhance focal adhesions. In addition, histone Kla might activate many LUAD tumorigenesis and progression-related pathways, such as the MAPK signaling pathway [55], VEGF signaling pathway [56], and NOTCH signaling pathway [57]. Moreover, the activation of these signaling pathways is related to the therapy resistance of LUAD [55, 58]. Hence, targeting Kla may impair the activation of these LUAD-associated pathways, suggesting that Kla was expected to be a novel therapeutic target for LUAD.

5. Limitations

However, despite the vital clinical importance of the study, there are several limitations. Firstly, further determination of the expression of prognostic biomarkers in LUAD specimens is warranted. Additionally, more in vitro and in vivo studies are needed to explore the role of Kla in immunotherapy and chemotherapy.

6. Conclusion

Histone Kla was related to prognosis of patients with LUAD, and was identified as an independent biomarker. Meanwhile, Kla activation enhanced Tregs, TAMs infiltration and decreased NK cells level in LUAD immune microenvironment. In addition, histone Kla might inhibit the LUAD immune process, and thereby contributed to immunotherapy

resistance. Moreover, activation of Kla might induce focal adhesion, MARK, NOTCH and VEGF signaling pathways, which are all related to tumorigenesis, metastasis, and therapy resistance. These findings suggested that Kla might be a critical therapeutic target for LUAD.

Abbreviations

LUAD	Lung Adenocarcinoma
Kla	Lysine Lactylation
TCGA	The Cancer Genome Atlas
DEKlaGs	Differentially Expressed Kla-specific Genes
GSEA	Gene set Enrichment Analysis
KEGG	Kyoto Encyclopedia of Genes and Genomes
P300	E1A Binding Protein p300
HIF1A	Hypoxia Inducible Factor 1 Subunit Alpha
LAHA/B	Lactate Dehydrogenase A/B
TME	Tumor Microenvironment
TMB	Tumor Mutation Burden
C1QNTF6	C1q and TNF-related 6
HCN2	Hyperpolarization-activated Cyclic Nucleotide Gated Potassium and Sodium Channel 2
IL20RB	Interleukin 20 Receptor Subunit Beta
SLAMF9	SLAM Family Member 9
ICB	Immune Checkpoint Blocking

Author Contributions

Yi Zhang: Software, Formal analysis, Writing – original draft, Writing – review & editing

Jianhong Ren: Writing – original draft, Writing – review & editing

Guangzhao Huang: Formal analysis

Rurong Wang: Conceptualization, Supervision, Writing – review & editing, Funding acquisition

Declarations

Ethical Approval

All of data in our study were obtained from public database. So, ethical approval and informed consent were not required in our study.

Consent for Publication

All authors have revised and agreed to publish this manuscript.

Funding

None.

Data Availability Statement

The data in this study were obtained from the following websites: https://portal.gdc.cancer.gov/, https://www.ncbi.nlm.nih.gov/geo/, http://xena.ucsc.edu/, https://discover.nci.nih.gov/cellminer/home.do, https://www.gsea-msigdb.org/gsea/index.jsp, https://www.proteinatlas.org/, https://tcia.at/home. All of the data presented in this study could be obtained from corresponding author.

Conflicts of Interest

All of authors declare no conflict of interest.

Appendix

Table A1. *Differentially expressed Kla-specific genes in LUAD.*

Gene	logFC	pValue	FDR	gene	logFC	pValue	FDR
A1CF	4.3774	0.0031	0.0042	MAMDC2	-2.6703	0.0000	<0.0001
ACVRL1	-2.6073	0.0000	<0.0001	MARCO	-3.0003	0.0000	<0.0001
ADGB	-2.1778	0.0001	<0.0001	MMP10	4.1263	0.0000	<0.0001
AIM2	2.8949	0.0000	<0.0001	NAT8L	3.4705	0.0000	<0.0001
C1QTNF6	2.2639	0.0000	<0.0001	NECTIN4	2.3959	0.0000	<0.0001
CASP12	-2.4928	0.0000	<0.0001	NKAIN1	4.9290	0.0000	<0.0001
CAV1	-3.4012	0.0000	<0.0001	OCIAD2	2.2174	0.0000	<0.0001

Gene	logFC	pValue	FDR	gene	logFC	pValue	FDR
CCL24	-2.4561	0.0000	<0.0001	OLR1	-2.4468	0.0000	<0.0001
CD101	-2.6523	0.0000	<0.0001	OVOL1	2.3245	0.0000	<0.0001
CD36	-2.9461	0.0000	<0.0001	PABPC1L	2.0961	0.0000	<0.0001
CELSR3	3.4629	0.0000	<0.0001	PADI4	-2.5395	0.0000	<0.0001
CGNL1	-2.1863	0.0000	<0.0001	PERM1	2.6740	0.0000	<0.0001
COL11A2	2.8228	0.0404	0.0472	PI16	-3.6922	0.0000	<0.0001
CP	3.6776	0.0000	<0.0001	PKIB	2.1181	0.0000	<0.0001
CSF3	-4.7763	0.0000	<0.0001	PLPP2	2.4194	0.0000	<0.0001
DACH1	-2.4866	0.0000	<0.0001	PLXNB3	3.3313	0.0001	<0.0001
DIO2	2.4893	0.0000	<0.0001	PPFIA4	2.4639	0.0000	<0.0001
DNMT3B	2.1207	0.0000	<0.0001	PRKCG	2.2884	0.0000	<0.0001
DUSP9	4.6763	0.0000	<0.0001	PRX	-3.4083	0.0000	<0.0001
EDNRB	-3.5082	0.0000	<0.0001	PTPRN	4.4711	0.0001	<0.0001
EFNA2	5.9205	0.0000	<0.0001	PYCR1	3.7351	0.0000	<0.0001
EGLN3	2.9836	0.0000	<0.0001	RCOR2	2.7510	0.0000	<0.0001
FABP4	-4.8672	0.0000	<0.0001	RGCC	-2.9318	0.0000	<0.0001
FADS6	5.2795	0.0000	<0.0001	RNASE10	2.6753	0.0000	<0.0001
FGF11	3.4319	0.0000	<0.0001	RUNDC3A	2.3011	0.0015	0.0020
FGR	-2.1110	0.0000	<0.0001	SELP	-2.3894	0.0000	<0.0001
GALR3	3.4530	0.0000	<0.0001	SLAMF9	2.0117	0.0001	<0.0001
GINS4	2.5369	0.0000	<0.0001	SLC6A4	-6.1557	0.0000	<0.0001
GNG4	4.5860	0.0000	<0.0001	SLC7A5	2.7328	0.0000	<0.0001
GPX3	-2.2846	0.0000	<0.0001	SMIM24	4.0765	0.0000	<0.0001
GSTA3	-2.6316	0.0000	<0.0001	ST18	2.5851	0.0002	<0.0001
HAS1	-3.4969	0.0000	<0.0001	SUSD2	-2.0427	0.0000	<0.0001
HBEGF	-2.5640	0.0000	<0.0001	TGM1	-2.4943	0.0000	<0.0001
HCN2	2.3544	0.0000	<0.0001	TMEM82	4.9259	0.0000	<0.0001
IL1RL1	-2.8850	0.0000	<0.0001	TNNT1	3.2432	0.0001	<0.0001
IL1RL2	2.3052	0.0000	<0.0001	TNS1	-2.1434	0.0000	<0.0001
IL20RB	3.8372	0.0000	<0.0001	TPPP3	-2.2937	0.0000	<0.0001
ITM2A	-2.0584	0.0000	<0.0001	TUBB2B	4.0907	0.0000	<0.0001
JAM2	-2.5399	0.0000	<0.0001	TUBB3	4.4679	0.0000	<0.0001
KCNJ10	2.1032	0.0000	<0.0001	TUBB4A	2.3612	0.0129	0.0160
KIF5A	2.8963	0.0000	<0.0001	VGF	6.1278	0.0000	<0.0001
LBP	4.6866	0.0042	0.0056	VWF	-2.3626	0.0000	<0.0001
LIMS2	-2.8768	0.0000	<0.0001	WNT6	2.0001	0.0000	<0.0001

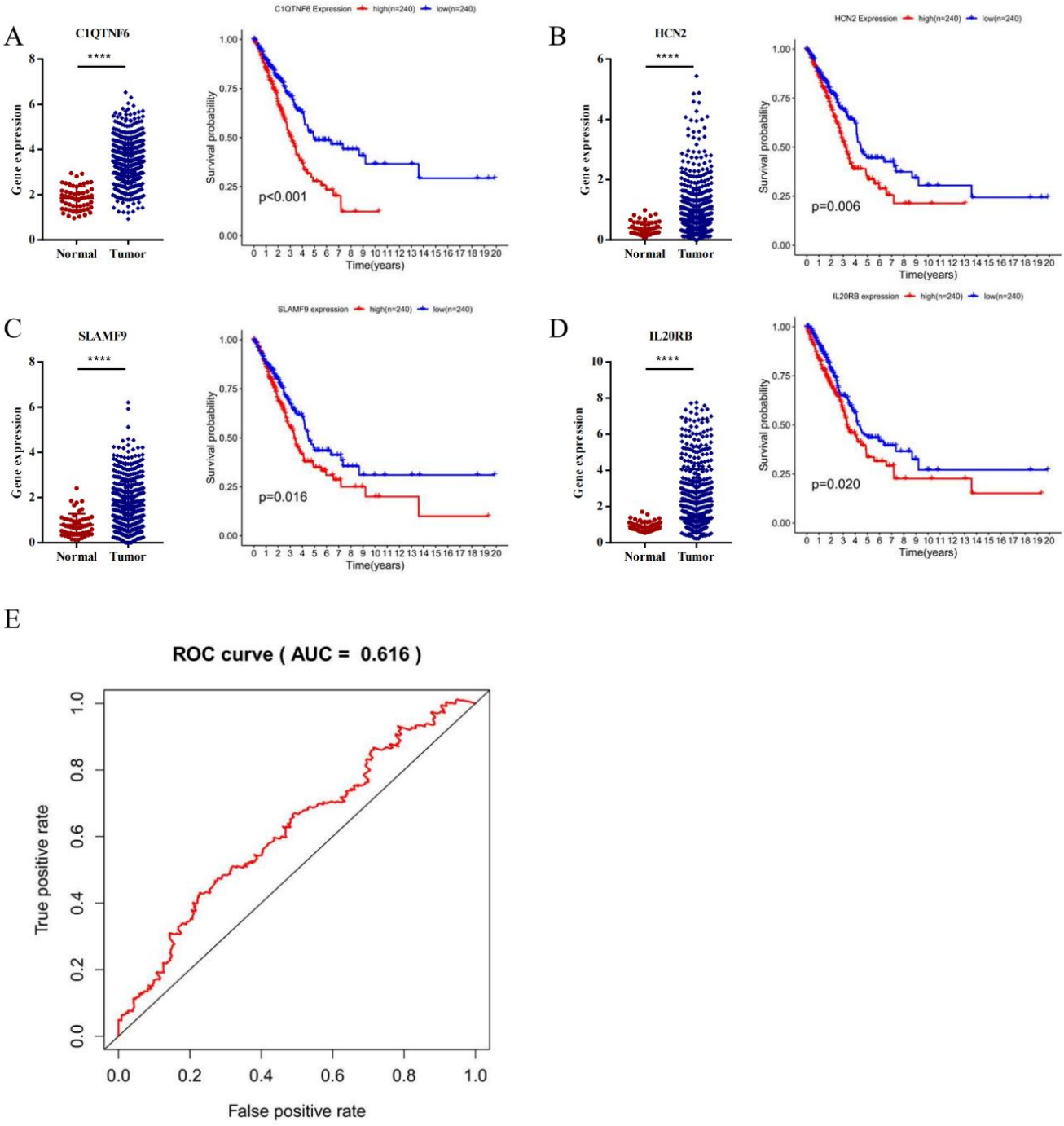

Figure A1. *The prognostic value of Kla-specific genes enrolled on Cox regression model. A; B; C; D, C1QTNF6, HCN2, SLAMF9 and IL20RB were all overexpression in LUAD tumor tissues, and correlated with poor overall survival rate. E, The Receiver Operating Characteristic (ROC) curve of Cox regression model. Area Under Curve (AUC) is 0.616.*

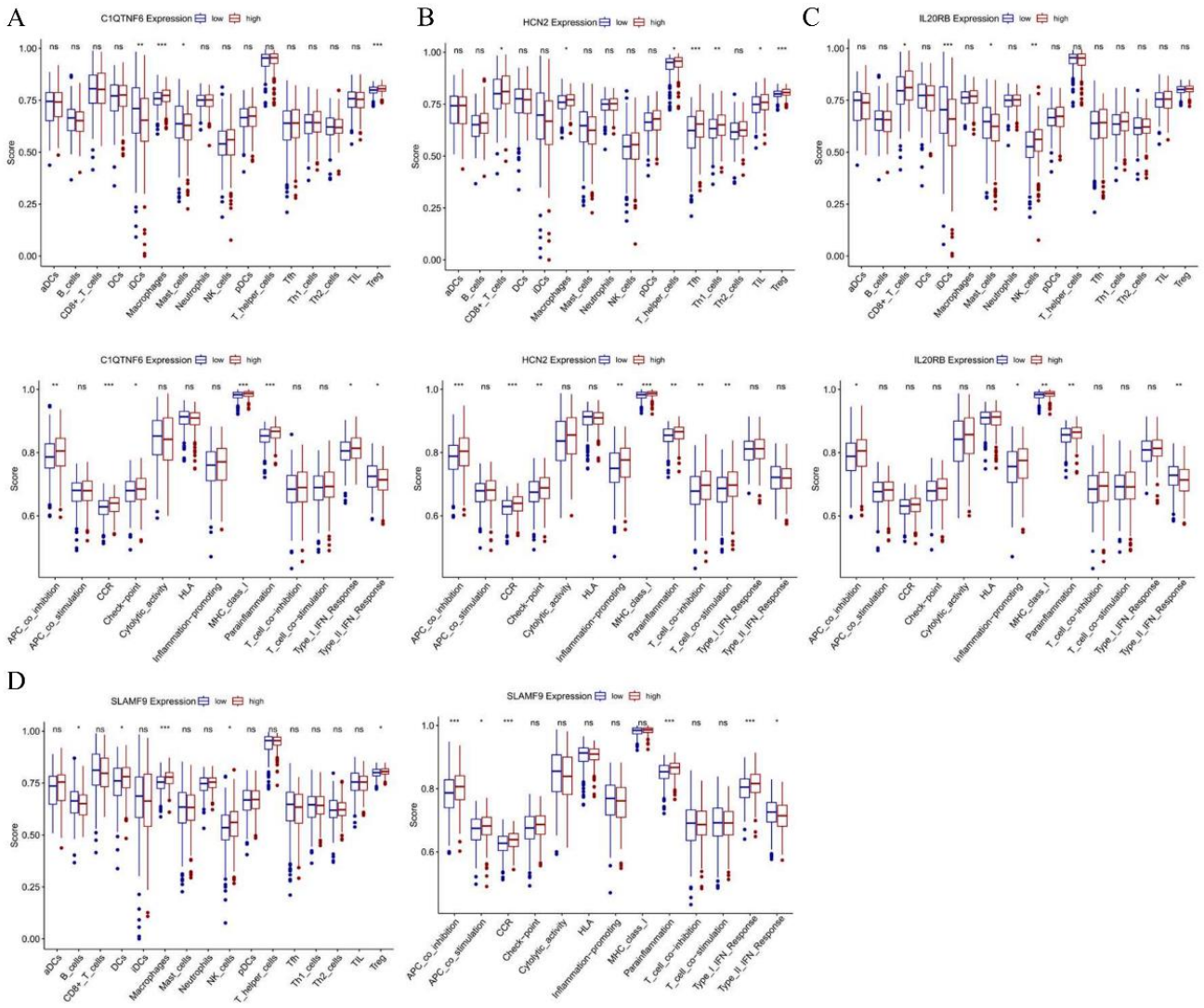

Figure A2. *The role of Kla-specific genes on LUAD TME. A, High C1QTNF6 expression was associated with elevated Treg level and low Type-2 IFN response. B, HCN2 might played a crucial role in regulating the function of follicular helper T cell (Tfh) and enhanced Treg function. C, SLAMF9 mainly regulated the different stages of Macrophages and promoted Treg function. SLAMF9 also inhibited the Type-2 IFN response. D, the correlation between IL20RB and immune cell, immune function scores.*

Table A2. *Correlation between C1QTNF6 and drug susceptibility.*

Drug	cor	pvalue
Carfilzomib	-0.4449	0.0004
Pipamperone	-0.4188	0.0009
Vincristine	-0.4107	0.0011
Ixazomib citrate	-0.4033	0.0014
Paclitaxel	-0.3596	0.0048
Dolastatin 10	-0.3427	0.0074
PX-316	-0.3377	0.0083
Eribulin mesilate	-0.3312	0.0097
Nilotinib	-0.3263	0.0110

Drug	cor	pvalue
Bortezomib	-0.2935	0.0228
okadaic acid	-0.2913	0.0240
Tyrothricin	-0.2885	0.0254
Dimethylaminoparthenolide	-0.2828	0.0286
Crizotinib	-0.2810	0.0297
Vinblastine	-0.2763	0.0326
Ethinyl estradiol	-0.2707	0.0365
Obatoclax	-0.2694	0.0374
BML-277	-0.2660	0.0399
Carmustine	-0.2656	0.0403
Chelerythrine	-0.2603	0.0446
Arsenic trioxide	-0.2591	0.0456

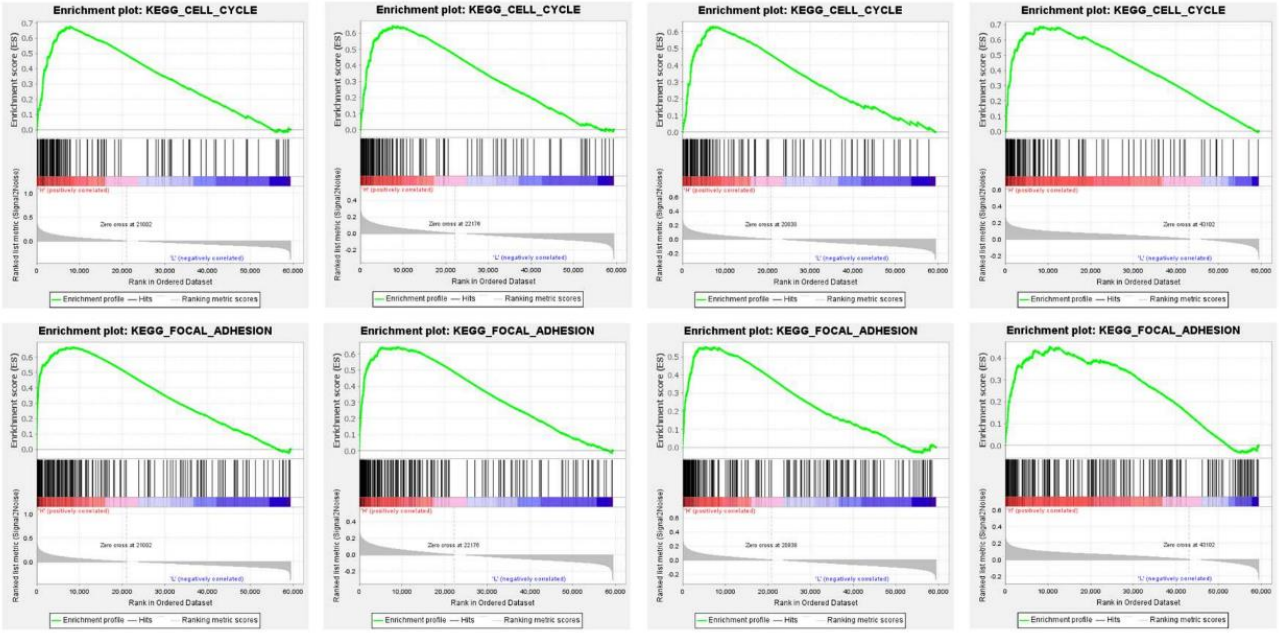

Figure A3. *Prognostic Kla-specific genes induced LUAD cell cycle and focal adhesion.*

Table A3. *Correlation between HCN2 and drug susceptibility.*

Drug	cor	pvalue
3-Bromopyruvate (acid)	-0.4389	0.0005
Hypothemycin	-0.4314	0.0006
Obatoclax	-0.3990	0.0016
Parthenolide	-0.3740	0.0032
Selumetinib	-0.3057	0.0176
Cobimetinib (isomer 1)	-0.2965	0.0214

Drug	cor	pvalue
Fostamatinib	-0.2856	0.0270
Imexon	-0.2798	0.0304
Palbociclib	-0.2698	0.0371
Sunitinib	-0.2652	0.0406
Dimethylaminoparthenolide	-0.2606	0.0443
PX-316	-0.2579	0.0466
Perifosine	-0.2559	0.0485

Table A4. *Correlation between SLAMF9 and drug susceptibility.*

Drug	cor	pvalue
LMP776	-0.4064	0.0013
Pyrazoloacridine	-0.4062	0.0013
Clofarabine	-0.3654	0.0041
Mitoxantrone	-0.3568	0.0051
O-6-Benzylguanine	-0.3171	0.0135
Batracylin	-0.3158	0.0140
AP-26113	-0.2994	0.0201
Dasatinib	-0.2957	0.0218
Staurosporine	-0.2775	0.0318
Idarubicin	-0.2773	0.0319
Midostaurin	-0.2745	0.0338
Bleomycin	-0.2703	0.0367
Gemcitabine	-0.2617	0.0434
Docetaxel	-0.2576	0.0469
RH1	-0.2555	0.0488
Irinotecan	-0.2553	0.0490

Table A5. *Correlation between IL20RB and drug susceptibility.*

Drug	cor	pvalue
Tamoxifen	-0.4683	0.0002
Tanespimycin	-0.3787	0.0029
Bosutinib	-0.3320	0.0096
geldanamycin analog	-0.3177	0.0134
Alvespimycin	-0.2852	0.0272

References

[1] Sung, H., Ferlay, J., Siegel, R. L. et al: Global Cancer Statistics 2020: GLOBOCAN Estimates of Incidence and Mortality Worldwide for 36 Cancers in 185 Countries. CA Cancer J Clin. 2021; 71(3): 209-249.

[2] Vokes, N. I., Pan, K., Le, X.: Efficacy of immunotherapy in oncogene-driven non-small-cell lung cancer. Ther Adv Med Oncol. 2023; 15: 17588359231161409.

[3] Scalera, S., Mazzotta, M., Corleone, G. et al: KEAP1 and TP53 Frame Genomic, Evolutionary, and Immunologic Subtypes of Lung Adenocarcinoma With Different Sensitivity to Immunotherapy. J Thorac Oncol. 2021; 16(12): 2065-2077.

[4] Skoulidis, F., Goldberg, M. E., Greenawalt, D.M. et al: STK11/LKB1 Mutations and PD-1 Inhibitor Resistance in KRAS-Mutant Lung Adenocarcinoma. Cancer Discov. 2018; 8(7): 822-835.

[5] Walder, D., O'Brien, M.: Looking back and to the future: Are we improving 'cure' in non-small cell lung cancer? Eur J Cancer. 2017; 75: 192-194.

[6] Robusti, G., Vai, A., Bonaldi, T. et al: Investigating pathological epigenetic aberrations by epi-proteomics. Clin Epigenetics. 2022; 14(1): 145.

[7] Audia, J. E., Campbell, R. M.: Histone Modifications and Cancer. Cold Spring Harb Perspect Biol. 2016; 8(4): a019521.

[8] Khan, S. A., Reddy, D., Gupta, S.: Global histone post-translational modifications and cancer: Biomarkers for diagnosis, prognosis and treatment? World J Biol Chem. 2015; 6(4): 333-345.

[9] Zhang, D., Tang, Z., Huang, H. et al: Metabolic regulation of gene expression by histone lactylation. Nature. 2019; 574(7779): 575-580.

[10] Lv, X., Lv, Y., Dai, X.: Lactate, histone lactylation and cancer hallmarks. Expert Rev Mol Med. 2023; 25: e7.

[11] Chen, L., Huang, L., Gu, Y. et al: Lactate-Lactylation Hands between Metabolic Reprogramming and Immunosuppression. Int J Mol Sci. 2022; 23(19).

[12] Fan, H., Yang, F., Xiao, Z. et al: Lactylation: novel epigenetic regulatory and therapeutic opportunities. Am J Physiol Endocrinol Metab. 2023; 324(4): E330-e338.

[13] Warburg, O.: On the origin of cancer cells. Science. 1956; 123(3191): 309-314.

[14] Yu, J., Chai, P., Xie, M. et al: Histone lactylation drives oncogenesis by facilitating m(6)A reader protein YTHDF2 expression in ocular melanoma. Genome Biol. 2021; 22(1): 85.

[15] Wang, J., Liu, Z., Xu, Y. et al: Enterobacterial LPS-inducible LINC00152 is regulated by histone lactylation and promotes cancer cells invasion and migration. Front Cell Infect Microbiol. 2022; 12: 913815.

[16] Pan, L., Feng, F., Wu, J. et al: Demethylzeylasteral targets lactate by inhibiting histone lactylation to suppress the tumorigenicity of liver cancer stem cells. Pharmacol Res. 2022; 181: 106270.

[17] Liu, X. S., Zhou, L. M., Yuan, L. L. et al: NPM1 Is a Prognostic Biomarker Involved in Immune Infiltration of Lung Adenocarcinoma and Associated With m6A Modification and Glycolysis. Front Immunol. 2021; 12: 724741.

[18] Zhu, S., Chen, W., Wang, J. et al: SAM68 promotes tumorigenesis in lung adenocarcinoma by regulating metabolic conversion via PKM alternative splicing. Theranostics. 2021; 11(7): 3359-3375.

[19] Cao, F., Yang, D., Tang, F. et al: Girdin Promotes Tumorigenesis and Chemoresistance in Lung Adenocarcinoma by Interacting with PKM2. Cancers (Basel). 2022; 14(22).

[20] Zhang, P., Pei, S., Gong, Z. et al: The integrated single-cell analysis developed a lactate metabolism-driven signature to improve outcomes and immunotherapy in lung adenocarcinoma. Front Endocrinol (Lausanne). 2023; 14: 1154410.

[21] Wang, S., Zhang, M., Li, T. et al: A Comprehensively Prognostic and Immunological Analysis of PARP11 in Pan-cancer. J Leukoc Biol. 2024.

[22] Allgäuer, M., Budczies, J., Christopoulos, P. et al: Implementing tumor mutational burden (TMB) analysis in routine diagnostics-a primer for molecular pathologists and clinicians. Transl Lung Cancer Res. 2018; 7(6): 703-715.

[23] Wu, Q., Li, X., Long, M. et al: Integrated analysis of histone lysine lactylation (Kla)-specific genes suggests that NR6A1, OSBP2 and UNC119B are novel therapeutic targets for hepatocellular carcinoma. Sci Rep. 2023; 13(1): 18642.

[24] Chen, H., Luo, H., Wang, J. et al: Identification of a pyroptosis-related prognostic signature in breast cancer. BMC Cancer. 2022; 22(1): 429.

[25] Huang, P., Zhu, S., Liang, X. et al: Regulatory Mechanisms of LncRNAs in Cancer Glycolysis: Facts and Perspectives. Cancer Manag Res. 2021; 13: 5317-5336.

[26] Husain, Z., Huang, Y., Seth, P. et al: Tumor-derived lactate modifies antitumor immune response: effect on myeloid-derived suppressor cells and NK cells. J Immunol. 2013; 191(3): 1486-1495.

[27] Brand, A., Singer, K., Koehl, G. E. et al: LDHA-Associated Lactic Acid Production Blunts Tumor Immunosurveillance by T and NK Cells. Cell Metab. 2016; 24(5): 657-671.

[28] Xing, Y., Luo, P., Hu, R. et al: TRIB3 Promotes Lung Adenocarcinoma Progression via an Enhanced Warburg Effect. Cancer Manag Res. 2020; 12: 13195-13206.

[29] Makinoshima, H., Takita, M., Saruwatari, K. et al: Signaling through the Phosphatidylinositol 3-Kinase (PI3K)/Mammalian Target of Rapamycin (mTOR) Axis Is Responsible for Aerobic Glycolysis mediated by Glucose Transporter in Epidermal Growth Factor Receptor (EGFR)-mutated Lung Adenocarcinoma. J Biol Chem. 2015; 290(28): 17495-17504.

[30] Zhao, F., Wang, Z., Li, Z. et al: Identifying a lactic acid metabolism-related gene signature contributes to predicting prognosis, immunotherapy efficacy, and tumor microenvironment of lung adenocarcinoma. Front Immunol. 2022; 13: 980508.

[31] Liu, W., Zhang, J., Xie, T. et al: C1QTNF6 is a Prognostic Biomarker and Related to Immune Infiltration and Drug Sensitivity: A Pan-Cancer Analysis. Front Pharmacol. 2022; 13: 855485.

[32] Iglesias-Escudero, M., Arias-Gonz ález, N., Mart ínez-C áceres, E.: Regulatory cells and the effect of cancer immunotherapy. Mol Cancer. 2023; 22(1): 26.

[33] Zhu, H., Zheng, C., Liu, H. et al: Significance of macrophage infiltration in the prognosis of lung adenocarcinoma patients evaluated by scRNA and bulkRNA analysis. Front Immunol. 2022; 13: 1028440.

[34] Chen, S., Zhang, J., Li, Q. et al: A Novel Secreted Protein-Related Gene Signature Predicts Overall Survival and Is Associated With Tumor Immunity in Patients With Lung Adenocarcinoma. Front Oncol. 2022; 12: 870328.

[35] Zhu, C., Xie, Y., Li, Q. et al: CPSF6-mediated XBP1 3'UTR shortening attenuates cisplatin-induced ER stress and elevates chemo-resistance in lung adenocarcinoma. Drug Resist Updat. 2023; 68: 100933.

[36] Lin, G., Lin, L., Lin, H. et al: C1QTNF6 regulated by miR-29a-3p promotes proliferation and migration in stage I lung adenocarcinoma. BMC Pulm Med. 2022; 22(1): 285.

[37] Cai, S., Zhang, B., Huang, C. et al: CTRP6 protects against ferroptosis to drive lung cancer progression and metastasis by destabilizing SOCS2 and augmenting the xCT/GPX4 pathway. Cancer Lett. 2023; 579: 216465.

[38] Mok, K. C., Tsoi, H., Man, E. P. et al: Repurposing hyperpolarization-activated cyclic nucleotide-gated channels as a novel therapy for breast cancer. Clin Transl Med. 2021; 11(11): e578.

[39] Calpe, S., Wang, N., Romero, X. et al: The SLAM and SAP gene families control innate and adaptive immune responses. Adv Immunol. 2008; 97: 177-250.

[40] Huang, Y., Shan, G., Yi, Y. et al: FSCN1 induced PTPRF-dependent tumor microenvironment inflammatory reprogramming promotes lung adenocarcinoma progression via regulating macrophagic glycolysis. Cell Oncol (Dordr). 2022; 45(6): 1383-1399.

[41] Hu, R., Xu, B., Ma, J. et al: LINC00963 promotes the malignancy and metastasis of lung adenocarcinoma by stabilizing Zeb1 and exosomes-induced M2 macrophage polarization. Mol Med. 2023; 29(1): 1.

[42] Zeng, X., Liu, G., Peng, W. et al: Combined deficiency of SLAMF8 and SLAMF9 prevents endotoxin-induced liver inflammation by downregulating TLR4 expression on macrophages. Cell Mol Immunol. 2020; 17(2): 153-162.

[43] Dollt, C., Michel, J., Kloss, L. et al: The novel immunoglobulin super family receptor SLAMF9 identified in TAM of murine and human melanoma influences pro-inflammatory cytokine secretion and migration. Cell Death Dis. 2018; 9(10): 939.

[44] He, J., Zhong, Y., Sun, Y. et al: Construction of an immune-related prognostic model by exploring the tumor microenvironment of clear cell renal cell carcinoma. Anal Biochem. 2022; 643: 114567.

[45] Yu, Z., Tang, H., Chen, S. et al: Exosomal LOC85009 inhibits docetaxel resistance in lung adenocarcinoma through regulating ATG5-induced autophagy. Drug Resist Updat. 2023; 67: 100915.

[46] Jiang, M., Qi, F., Zhang, K. et al: MARCKSL1-2 reverses docetaxel-resistance of lung adenocarcinoma cells by recruiting SUZ12 to suppress HDAC1 and elevate miR-200b. Mol Cancer. 2022; 21(1): 150.

[47] He, Y., Luo, W., Liu, Y. et al: IL-20RB mediates tumoral response to osteoclastic niches and promotes bone metastasis of lung cancer. J Clin Invest. 2022; 132(20).

[48] Zhang, S., Yang, G.: IL22RA1/JAK/STAT signaling acts as a cancer target through pan-cancer analysis. Front Immunol. 2022; 13: 915246.

[49] Zhang, M., Zhu, K., Pu, H. et al: An Immune-Related Signature Predicts Survival in Patients With Lung Adenocarcinoma. Front Oncol. 2019; 9: 1314.

[50] Fan, T., Pan, S., Yang, S. et al: Clinical Significance and Immunologic Landscape of a Five-IL(R)-Based Signature in Lung Adenocarcinoma. Front Immunol. 2021; 12: 693062.

[51] Kleczko, E. K., Kwak, J. W., Schenk, E. L. et al: Targeting the Complement Pathway as a Therapeutic Strategy in Lung Cancer. Front Immunol. 2019; 10: 954.

[52] Spella, M., Stathopoulos, G. T.: Immune Resistance in Lung Adenocarcinoma. Cancers (Basel). 2021; 13(3).

[53] Klempner, S. J., Fabrizio, D., Bane, S. et al: Tumor Mutational Burden as a Predictive Biomarker for Response to Immune Checkpoint Inhibitors: A Review of Current Evidence. Oncologist. 2020; 25(1): e147-e159.

[54] Chan, T. A., Yarchoan, M., Jaffee, E. et al: Development of tumor mutation burden as an immunotherapy biomarker: utility for the oncology clinic. Ann Oncol. 2019; 30(1): 44-56.

[55] Lin, X., Ye, R., Li, Z. et al: KIAA1429 promotes tumorigenesis and gefitinib resistance in lung adenocarcinoma by activating the JNK/ MAPK pathway in an m(6)A-dependent manner. Drug Resist Updat. 2023; 66: 100908.

[56] Li, D., Yang, W., Arthur, C. et al: Systems biology analysis reveals new insights into invasive lung cancer. BMC Syst Biol. 2018; 12(Suppl 7): 117.

[57] Zhang, M., Han, Y., Zheng, Y. et al: ZEB1-activated LINC01123 accelerates the malignancy in lung adenocarcinoma through NOTCH signaling pathway. Cell Death Dis. 2020; 11(11): 981.

[58] Yin, J. Z., Shi, X. Q., Wang, M. D. et al: Arsenic trioxide elicits anti-tumor activity by inhibiting polarization of M2-like tumor-associated macrophages via Notch signaling pathway in lung adenocarcinoma. Int Immunopharmacol. 2023; 117: 109899.